Electronic Supplementary Material (ESI) for Nanoscale.

Supplementary Materials for

Optically tunable ultra-fast resistive switching in lead-free methyl-ammonium bismuth iodide perovskite film

Swapnadeep Poddar†, Yuting Zhang†, Yiyi Zhu, Qianpeng Zhang, Zhiyong Fan*

Department of Electronic & Computer Engineering, The Hong Kong University of Science and Technology, Clear Water Bay, Kowloon, Hong Kong SAR, China.

*Corresponding author email: eezfan@ust.hk

†These authors contributed equally to this work.

Optical and material characterization of MBI thin film

The tauc plot obtained from the UV-Vis study (inset of **Fig.S1a**) of MBI thin film has been shown in **Fig.S1a**. It can be observed that the cutoff point of the tauc-plot indicates an optical bandgap (E_g) of ~2.1 eV for the polycrystalline MBI thin film perovskite. The UPS plot shown in **Fig.S1b** shows the first cutoff point ($E_{cutoff1}$=16.28 eV) and the inset plot demarcates the second cutoff point ($E_{cutoff2}$ = 0.8 eV). The energy gap between the source ionization energy (21.22 eV) and the first cutoff point denotes the position of the Fermi level or work function (WF) for MBI perovskite (4.94 eV from vacuum). The energy gap between the second cutoff point and the Fermi level referenced as zero denotes the energy gap between the Fermi level and the valence band maxima (VBM). Therefore the valence band maxima was calculated to be -(4.94 + 0.8) eV or 5.74 eV from vacuum or -5.84 eV to be precise. When the energy bandgap obtained from **Fig.S1a** was added to the VBM, we got the conduction band minima (CBM) to be -3.64 eV. Similar method of band structure evaluation have been used previously for MBI and other material systems.[1, 2]

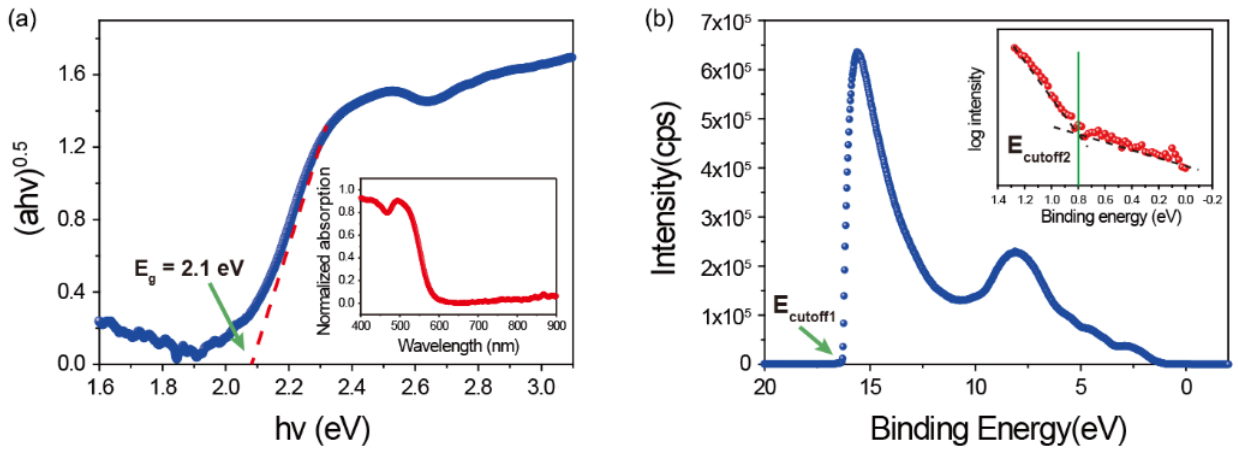

Fig.S1 Optical and material characterization of MBI thin film. (a) Tauc-plot showing the optical bandgap of MBI perovskite to be 2.1 eV. Inset shows the UV-Vis plot of MBI perovskite thin-film. (b) UPS plot showing the primary and secondary (in inset) electron cutoff-regions.

Device to device variation for electrical switching

The device to device variation for the MBI Re-RAM devices, shown in **Fig.S2**, were collected from individual devices having area 0.0016 mm^2. Stabilized *I-V* sweeps were run for each device from 0 V→ 8 V→ -8 V→ 0 V. The reading voltage used for tracing the LRS and HRS current was 0.1 V.

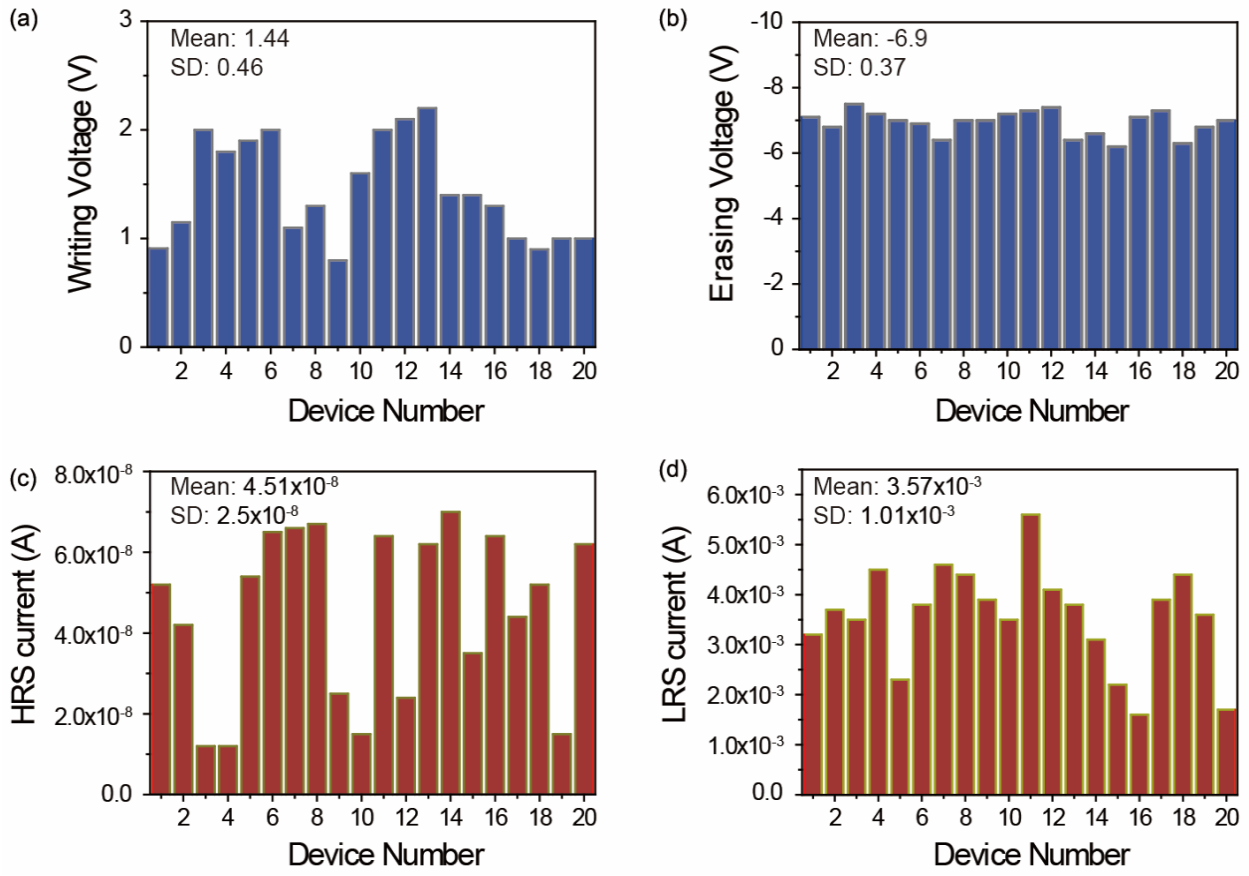

Fig.S2. Device to device variation for MBI Re-RAM. (a) Plot showing the variation of writing voltage for MBI Re-RAM. (b) Plot showing the variation of erasing voltage for MBI Re-RAM. (c) Plot showing the variation of HRS current values for MBI Re-RAM. (d) Plot showing the variation of LRS current values for MBI Re-RAM.

Cumulative density function for device endurance in MBI Re-RAM

The device endurance data presented in **Fig.3a** of manuscript was used for plotting the cumulative density function (CDF). It is to be noted that initial data points for 1730 cycles (sorted in ascending order) were chosen from the 2550 cycles shown in **Fig.3a** while plotting the CDF for LRS and HRS resistances. It was done so, as after 1730 cycles, the LRS began its transformation to HRS. As shown in **Fig.S3**, the HRS and LRS showed excellent endurance characteristics for 1730 cycles without any significant degradation of ON/OFF ratio.

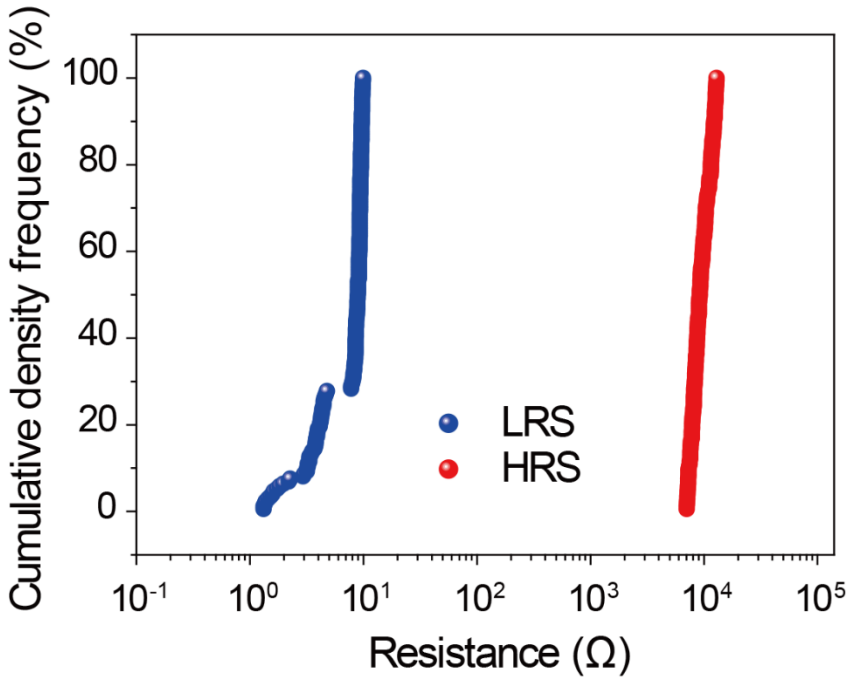

Fig.S3. Cumulative Density Function for device endurance in MBI Re-RAM

Pulse response of MBI Re-RAM

Pulse train comprising read/write/read/erase/read pulses of amplitude 0.1 V/ 7 V/ 0.1 V/- 10 V/ 0.1 V, 0.1 V/ 8 V/ 0.1 V/ -11 V/ 0.1 V, 0.1 V/ 9 V/ 0.1 V/ -10 V/ 0.1 V and 0.1 V/ 10 V/ 0.1 V/ -10 V/ 0.1 V was used to obtain distinctly different LRSs after writing with pulses of varying amplitude. The LRS current values thus traced after writing 7 V, 8 V, 9 V and 10 V were 0.55 mA, 0.82 mA, 1.17mA and 1.8mA respectively as shown in **Fig.S4**.

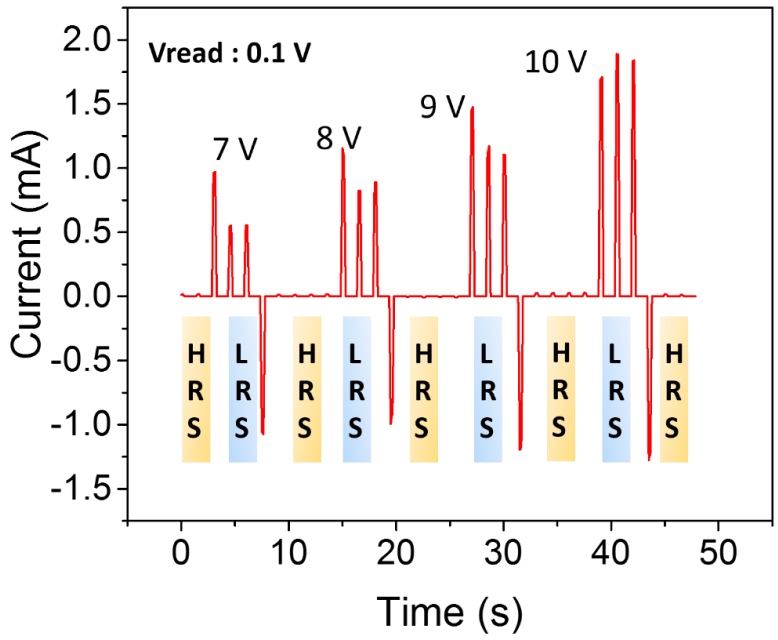

Fig.S4. Electrical pulse response in MBI Re-RAM demonstrating multi-bit storage capability.

Opto-electric memorization in MBI Re-RAM

In **Fig.S5a**, the temporal retention of the LRS current obtained by opto-electric stimulation (0.5 V DC bias and 100 mW/cm^2 intensity light for 20s) is plotted. The MBI Re-RAM showed a jump from LRS to HRS at ~ 1.1×10^4 s. Also, in **Fig.S5b,** it can be seen that upon prolonged illumination of 100 mW/cm^2 light over 100s, the LRS of the device transformed to HRS gradually. This indicates that the Joule heating resulting from high intensity illumination makes the LRS unstable to the extent where it can completely transform to HRS.

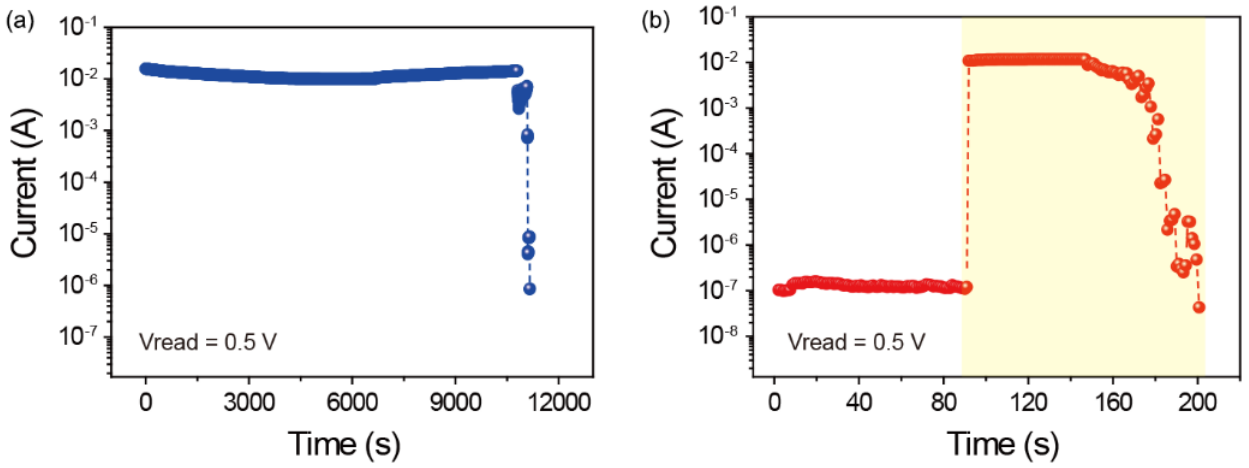

Fig.S5. Opto-electric memorization in MBI Re-RAM. (a) Plot showing temporal retention of opto-electrically achieved LRS current. (b) Plot showing degradation of LRS obtained by opto-electrical switching upon prolonged illumination by 100 mW/cm^2 intensity light source.

Device to device variation for opto-electric switching

The device to device variation for the MBI Re-RAM devices, shown in **Fig.S6**, were collected from individual devices having area 0.0016 mm^2. Stabilized *I-V* sweeps were run for each device from 0 V→ 8 V→ -8 V→ 0 V under 100 mW/cm^2 illumination to obtain the variation of writing and erasing voltage. The LRS and HRS current were extracted from the DC biasing test with readout voltage of 0.5 V, same as **Fig.4c** of main-text.

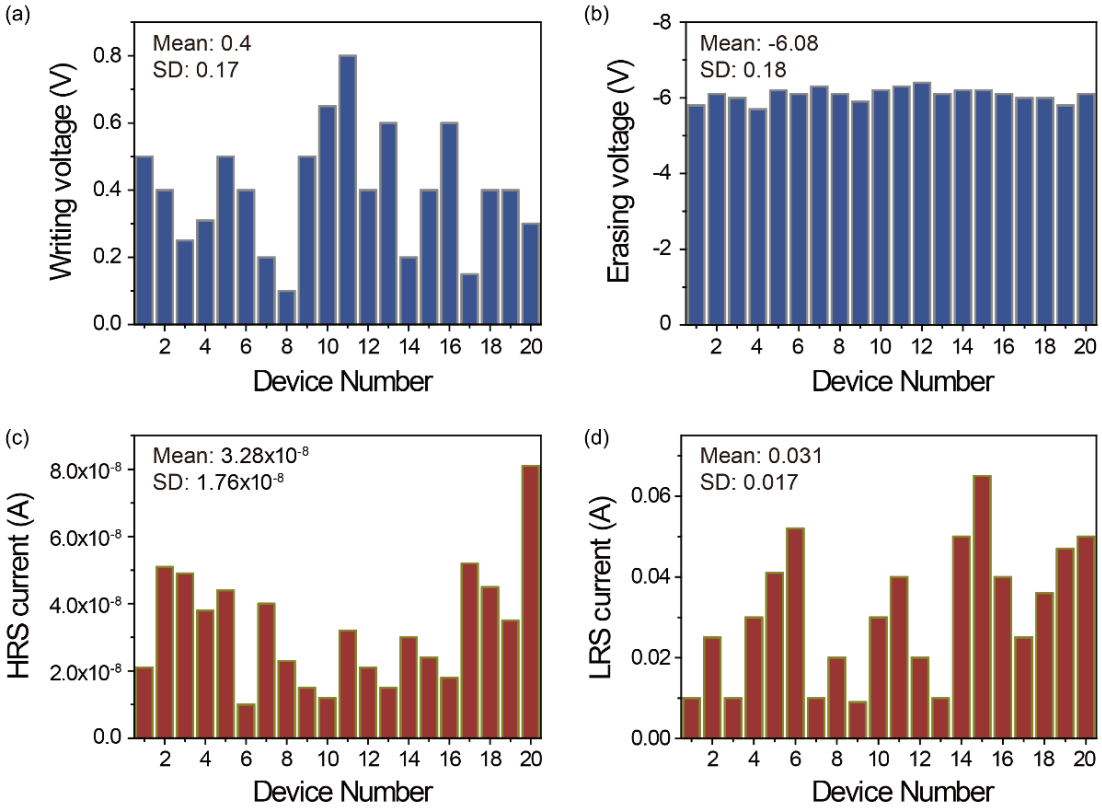

Fig.S6. Device to device variation for opto-electric switching. (a) Plot showing the variation of writing voltage under illumination. (b) Plot showing the variation of erasing voltage under illumination. (c) Plot showing the variation of HRS current values for opt-electric switching. (d) Plot showing the variation of LRS current values for opto-electric switching.

References

1. C. Momblona, H. Kanda, A. A. Sutanto, M. Mensi, C. Roldán-Carmona and M. K. Nazeeruddin, *Scientific Reports*, 2020, **10**, 1-8.
2. A. Agresti, A. Pazniak, S. Pescetelli, A. Di Vito, D. Rossi, A. Pecchia, M. A. der Maur, A. Liedl, R. Larciprete and D. V. Kuznetsov, *Nature Materials*, 2019, **18**, 1228-1234.